Deposition and characterization of carbon nanotubes on porous silicon by PECVD

M. A. Abed[a], M. M. Uonis[b*], G. G. Ali[c], I. B. Karomi[d]
[a]*Department of Physics, Faculty of Science, University of Mosul, Mosul 41002, Iraq*
[b]*New and Renewable Energies Department, Faculty of Science, University of Mosul, Iraq*
[c]*Physics Department, College of Education for Pure Science, Mosul University, Iraq*
[d]*Physics Department, College of Education for Pure Science, Mosul University, Iraq*

Nano porous silicon was achieved by electrochemical etching technique of current density 20 mA/cm ^{2}, 25% HF and etching time 15min. Carbon Nano layers have been deposited on PSi substrate by PECVD. XRD spectrum show that porous silicon has crystalline phase and becomes very broad after etching time, in addition, XRD spectrum for carbon layers show several peaks between (2θ=28.25-28.75) which belong to carbon nanotube and these peaks intensity increases with increasing of carbon thickness. Raman spectrum illustrates that peak position was at 516.32nm for porous silicon prepared at etching time 15 min.

(Received November 29, 2022; Accepted February 14, 2023)

Keywords: Carbon nanotubes, Porous silicon, PECVD

1. Introduction

The most important nanostructures are carbon nanotubes, and their importance comes due to the great change that they have made with their use in all fields .Carbon nanotubes are originally two-way strips of graphene wrapped around a specific axis to form a cylindrical shape with a diameter ranging between (0.4-50nm), each carbon atom hybrid (sp^2) has three covalent bonds[1]. Many kinds of fabrication methods have been established to grow the CNTs, such as sol-gel, chemical vapor deposition (CVD), PECVD and laser ablation [2]. The manufacture and preparation of materials and devices with nanoscale dimensions is of great importance due to the clear and sometimes significant change in the structural and chemical properties of these materials[3,4]. The performance of the plasma enhanced chemical vapor deposition is a very promising method for the development of optoelectronic devices because of its significant feature and high quality. It can be seen, this technique can be formed of uniform layers with a regular distributed along the surface [5]. Last years, several works reported has studied carbon nanotubes on the PSi material due to an appropriate material for several applications like photovoltaic devices, photo detectors, waveguides and the optoelectronic devices [6]. The combinations of carbon nanotubes and PSi layer are more important because the deposition of high - quality carbon films on a porous silicon surface can provide a good matching of lattice constant [7]. This work carried out more insight of the growth carbon nanotubes on porous silicon involved in homogenous for the selection of an optima process. The results were studied by surface properties (SEM), Structural properties (XRD) and Raman spectroscopy.

* Corresponding author: mohmahnua@uomosul.edu.iq
https://doi.org/10.15251/DJNB.2023.181.235

2. Material methodology

A porous silicon structure was achieved using the electrochemical etching technique. A commercially available mirror-like p-type (111) oriented silicon wafer of thickness (508±15μm) and (1.5 - 4 Ω.cm) resistivity was used. In order to form excess holes on the p-type silicon, the samples were dipped into Hydrophobic acid and Ethanol solution. The HF contraction has been diluted by using absolute ethanoic solution (25%) HF and (99%) (C_2H_5OH) during the etching for 20 min by current density of (20 mA/cm^2). The power supply was applied by two parts, the upper part is a steel and the lower part is made of gold. Figure 1 represents the experiment setup for the electrochemical etching.

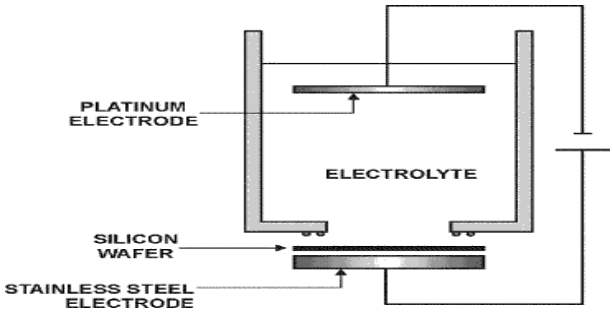

Fig. 1. Electrochemical etching system.

The carbon layer was deposited by plasma sputtering method with a precipitate current of 70A as the Figure 2. A pure Carbon rods was applied as a carbon source. The precipitation process was achieved in an atmosphere of argon gas. Porous Silicon wafers were used as a substrate to prepare the PSi-CNT structure [8]. Variable values of the plasma sputtering device that used for carbon deposition are shown in Table 1

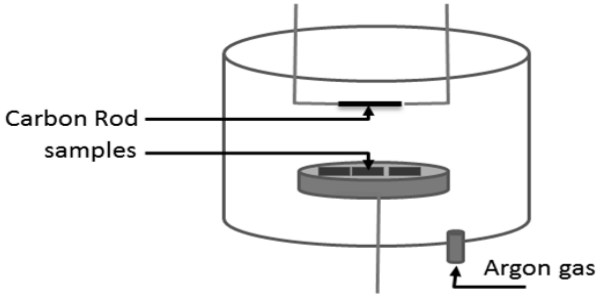

Fig. 2. Plasma sputtering system.

Table 1. Shows the values of the variables used in carbon deposition.

Parameter	Value
Pulse Current	70 A
Pulses Length	10 seconds
Number of Pulses	5
Out Gas Time	60 seconds
Out Gas Current	50 A

4. Results and discussion

Porous silicon substrate was prepared at the etching time 15min with 25 %HF and current density 20mA/cm^2. A sponge-like structure was produced during anodization process due to the extra chemical dissolution in HF and then to easy excess of holes at the top surface as shown in the Figure 3 [9]. The surface morphology of PSi can be strongly effect on the distribution between nearest neighbour pores. Thus, fabrication conditions can be used to control the final structures of PSi [10].

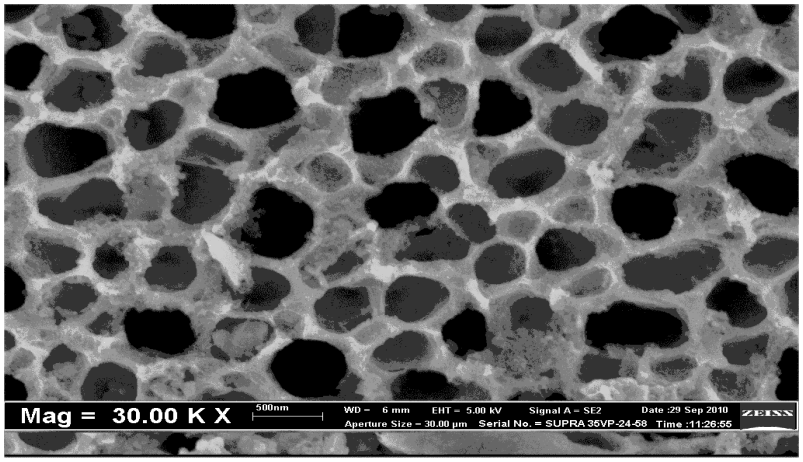

Fig. 3. SEM of porous silicon at etching time 15min.

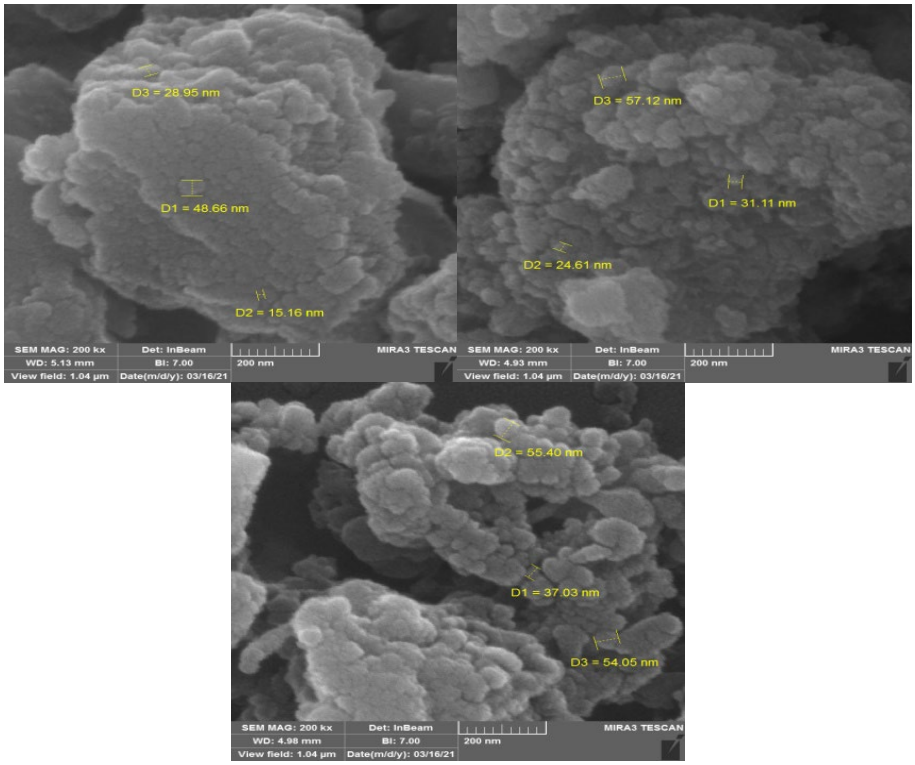

Fig. 4. Scanning electron microscope images for different carbon layer thickness (a:20nm, b:30nm and c:39nm).

Carbon layers with different thicknesses (20, 30 and 40 nm) have been deposited on the porous silicon substrates, scanning electron microscope images show that the grains with in the layers aggregate and grow with the increase of layers thicknesses as shown in Figure 4.

X-ray diffraction is another significant feature of the sample. Figure 5 shows that the porous silicon has single crystalline phase and sharp peak at 2θ = 28.2°, the value of hkl was found by JCDS card [11]. The pattern of the PSi remains crystalline phase, but it has a significant peak broadening with different at half maximum of full width due to formation of pores on silicon layer as in the Table 2. This confirms that the porous silicon has cubic structure [12]. Crystallites size can be calculated from Scherrer equation [13].

$$L = \frac{k\lambda}{B\cos\theta} \tag{1}$$

where L is grain crystallites (nm) and B is FWHM and k is a constant (k=0.894).

Table 2. Shows the values of FWHM, inter-plane distance and crystal size at time 15min.

Time(min.)	Crystallites size (nm)	FWHM (deg.)	d(°A)
15	10.78	1.134	2.173

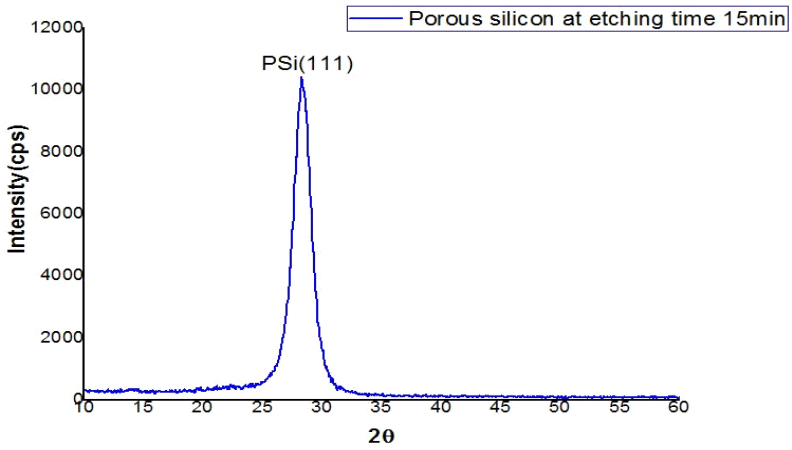

Fig. 5. X-ray spectrum of PSi formed at etching time 15min.

The X-ray spectrum of CNT-PSI structure shown in Figure 6, the strongest peaks was observed at 2θ = 28.25°, 28.75° and 28.3° for 40, 30 and 20 nm carbon thickness respectively. The both peaks in each spectrum belongs to the carbon nano tube [14,15,16]. It can be seen that the intensity of XRD increases with an increase thickness of film due to the carbon nanotube density with in the layers.

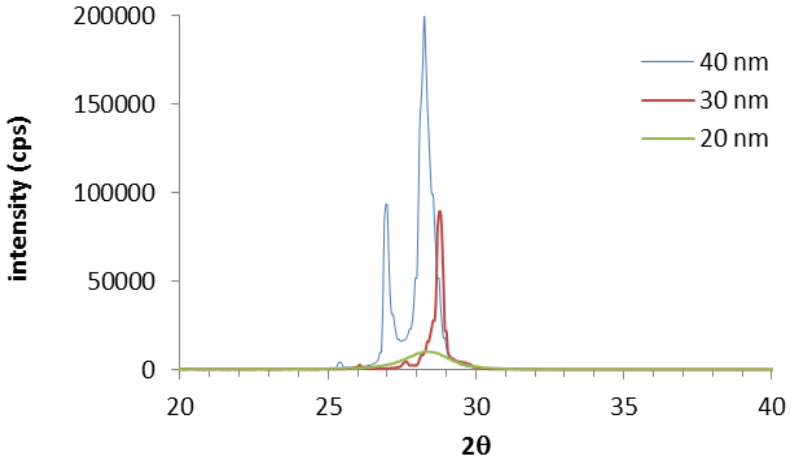

Fig. 6. X-ray spectrum of CNT-PSI structure for different carbon thickness (20,30 &40 nm).

Furthermore, the grain size increases with increasing carbon thickness due to formation of a small fraction of carbon leads to increase the fragmentation process [14,15].

Raman spectroscopy plays important role to determine the vibration properties of material. The Raman spectrum of bulk Si consists of a single sharp peak located at 520 cm^{-1}. Nano-porous silicon of Raman pattern exhibits extended shifted less 520 cm^{-1}. Figure 7 shows the shift of Raman peak position towards lower energies, this refers to the existence of nanostructure. As the crystalline size decreases, the optical phonon mode of PSi surface shifts to lower frequency and looks like asymmetry. The optical phonon is observed in the central of Brillouin zone [17, 18,19].

Table 2. Shows the values of FWHM, Raman Peak Position and Asymmetry for porous silicon with etching time 15min.

Etching time min	FWHM (cm^{-1})	Raman Peak Position (cm^{-1})	Asymmetry
15	17.3	516.32	1.6

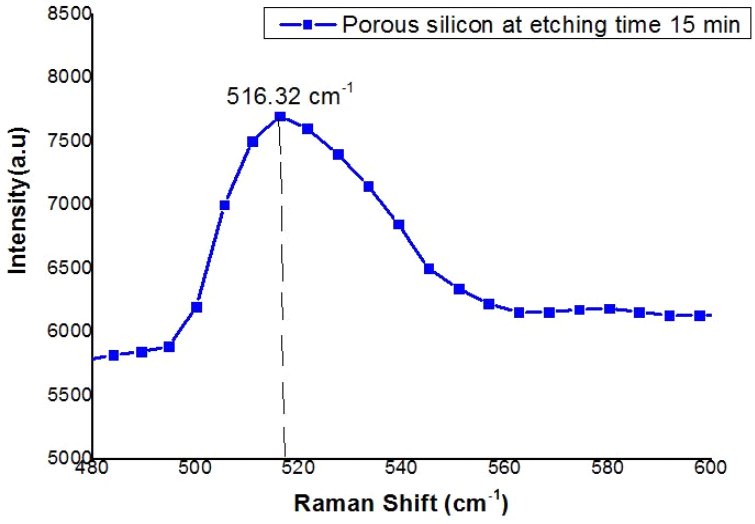

Fig. 7. Raman spectra of porous silicon at etching time 15min.

The significant proofs of the formation of carbon nanotubes is the Raman spectroscope. Figure 8 illustrates the Raman spectrum of a PSi-CNT device for 40nm carbon thickness with deposition current 70A. G peak of the crystalline phase of carbon appear within the wavelength range between (1580-1550 nm) and the appearance of the D peak of the amorphous phase of carbon within the wavelength range (1360-1350 nm) [20,21].The small displacement in the locations of the peaks is a result of increasing in the number of walls forming the carbon nanotubes, in other words, the increase in the diameter of these tubes with increase of the thickness of the carbon surface [22] .Moreover , we find that the intensity of the both peaks was slightly low, and we can explain this depending on the growth of carbon nanotubes formed within the carbon layer and the overlap between the spectra of porous silicon and carbon nanotubes.

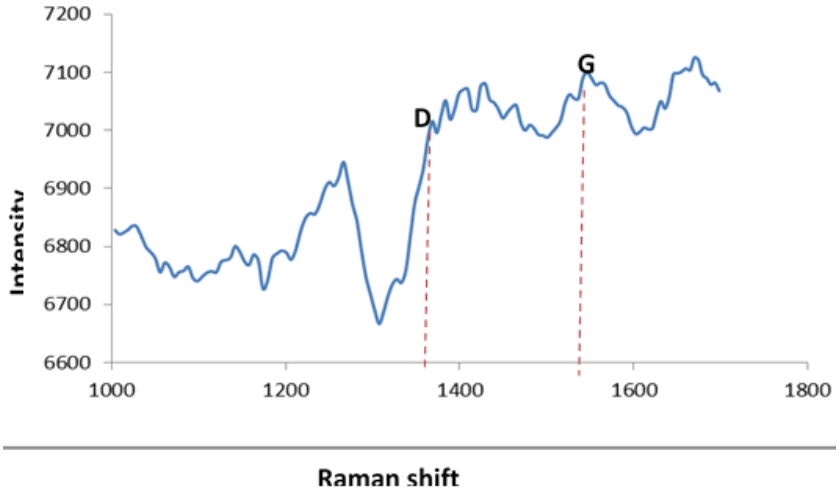

Fig. 8. Raman spectrum for PSi-CNT structure of 40nm carbon thickness.

5. Conclusion

A sponge-like structure was produced due to the extra chemical dissolution in HF and then to easy excess of holes.The distribution between nearest neighbour pores affected by surface morphology of porous silicon .Grain dimensions increase with carbon layer thickness. In the X-ray spectrum, single crystalline porous silicon has a sharp peak at $2\theta = 28.2°$ while the strongest peaks of CNT-PSI structure have been found at $2\theta = 28.25^{o}$, 28.75^{o} and 28.3^{o} for 40,30 and 20 nm carbon thickness respectively. Nano-porous silicon of Raman pattern exhibits extended shifted less 520 cm^{-1}. G and D peaks have been observed between (1580-1550 nm) and (1360-1350 nm) respectively and the small displacement in the position of both peaks are due to the increase in the carbon nanotubes walls numbers.

Acknowledgments

The authors would like to thank the College of Science, administration at Mosul University for supporting this work.

References

[1] Daniel Jay Hornbaker, Electronic Structure Of Carbon Nanotube Systems Measured With Scanning Tunneling Microscopy. Ph.D thesis, Physics in the Graduate College of the University of Illinois at Urbana-Champaign, Urbana, Illinois (2003).

[2] Behzad, K., Yunus, W.M., Talib, Z.A., Zakaria, A., Bahrami, A.and Shahriari, E. J. Mater., , 5(3):157-168(2012); https://doi.org/10.3390/ma5010157

[3] Kumar, P. Effect of Silicon Crystal Size on Photoluminescence Appearance in Porous Silicon. International Scholarly Research Network ISRN Nanotechnology. Article ID 163168, 2011;2(1) : 1-6; https://doi.org/10.5402/2011/163168

[4] Yasir Y. K., Ghazwan Gh. A., Marwan H.Y. Iraqi J. of Sci., 2021, 62(1), 130-137, https://doi.org/10.24996/ijs.2021.62.1.12

[5] Asli N. A., Suriani A. B., Shamsudin M. S., Yusop S. F., International Conference on Enabling Science and Nanotechnology.;3(2) (2012); https://doi.org/10.1109/ESciNano.2012.6149689

[6] Kan V.E., Bolotov V.V. , Ivlev K.E., Knyazev E.V. , Roslikov V.E., Procedia Engineering; 152(3):706-710(2016); https://doi.org/10.1016/j.proeng.2016.07.677

[7] R. A. Rasool , Ghazwan G. Ali , N. A. Hussein , Digest J. of Nanomaterials and Biostructures, 14, pp. 743 – 750, (2019).

[8] Ezzat A.M., Mustafa, B.M. and Uonis, M.M. Fabrication of Si-CNT Junction by Plasma Sputtering of Graphite Rods on Silicon Wafers. International Journal of Advanced Research; 2(1), 108-113(2014).

[9] Naderi N. and Hashim, M. , Effect of Surface Morphology on Electrical Properties of Electrochemically- Etching Porous Silicon Photodetectors . Int.J. Electrochem. Sci.; 7(3) :11512-11518(2012).

[10] Ou W. and Zhao L. Macroporous Silicon Fabrication by HF Electrochemical Etching for Antireflective Application in Solar Cell". International Journal of Materials and Mechanics Engineering; 1(1) (2012).

[11] Jayachandran M., Paramasivam M., Murali K.R. , Trivedi D.C. and Raghavan M. Synthesis of Porous Silicon Nanostructres for Photoluminescent Devices , Mater Phys; 4(2):143-147(2001).

[12] Lorusso A. , Nassisi V. , Congedo G., Lovergine N., Velardi L., Prete P., Applied Surface Science; 255 (3), 5401-5404(2009); https://doi.org/10.1016/j.apsusc.2008.08.030

[13] Russo L., Francesco C., Raffaele C.I. , laria R. , and Luca S. A Materials ; 4(1): 1023-1033(2015); https://doi.org/10.3390/ma4061023

[14]Muhammad F. Ramadhani , Maruli A. H. Pasaribu , Brian Yuliarto, Nugraha . AIP Conference Proceedings; 1586(74) (2014); https://doi.org/10.1063/1.4866733

[15] Taunk P.B. , Das R., Bisen D.P., Tamrakar R.K. , and Nootan R., Karbala International Journal of Modern Science ; 1(2) ,159-165(2015); https://doi.org/10.1016/j.kijoms.2015.11.002

[16] Wenzhen Li, Changhai L., Weijiang Z., Jieshan Q., Zhenhua Z., Gongquan S. and Qin X ., J. Phys. Chem. B,; 107(1) : 6292-6299(2003); https://doi.org/10.1021/jp022505c

[17] Ohmukai M., Nobutomo U., Tetsuya Y., and Yasuo T., Czechoslovak Journal of Physics; 54(7) : 781-784(2004); https://doi.org/10.1023/B:CJOP.0000038531.70434.dd

[18] Nesheva D. , Raptis C. , Perakis A. , Bineva, Z. , J. of Applied Physics; 92(8) : 4678-4683(2002); https://doi.org/10.1063/1.1504176

[19] Ghazwan Ghazi Ali , Abd UIKahliq A.S. , Marwan H. Y. ,Abidalkarem M. M., Results in Physics ; 14 (2) ,102466 (2019); https://doi.org/10.1016/j.rinp.2019.102466

[20] Valentinia L., Armentano I. , Kenny J. M. , Lozzi L. and Santucci S., Materials Letters ; 57(3) : 3699-3704(2003); https://doi.org/10.1016/S0167-577X(03)00166-6

[21] Laith R. , Ghazwan Gh . Ali, and Marwan H. Y. AIP Confer. Proceeding. 2201, 020001 (2019); https://doi.org/10.1063/1.5141425

[22] Bokova S. N., Obraztsova E. D. , Grebenyukov V. V., Elumeeva K. V. , Ishchenko A. V. and Kuznetsov V. L., Phys. Status Solidi B; 1(4) (2010); https://doi.org/10.1002/pssb.201000237